

Feasibility of measuring the Shapiro time delay over meter-scale distances

S Ballmer^{1,2,3}, S Márka⁴ and P Shawhan⁵

¹Syracuse University, Syracuse, NY 13244, USA

²TAMA - National Astronomical Observatory of Japan, Tokyo 181-8588, Japan

³LIGO - California Institute of Technology, Pasadena, CA 91125, USA

⁴Columbia University in the City of New York, New York, NY 10027, USA

⁵University of Maryland, College Park, MD 20742, USA

E-mail: sballmer@ligo.caltech.edu, smarka@phys.columbia.edu, pshawhan@umd.edu

Abstract. The time delay of light as it passes by a massive object, first calculated by Shapiro in 1964, is a hallmark of the curvature of space-time. To date, all measurements of the Shapiro time delay have been made over solar-system distance scales. We show that the new generation of kilometer-scale laser interferometers being constructed as gravitational wave detectors, in particular Advanced LIGO, will in principle be sensitive enough to measure variations in the Shapiro time delay produced by a suitably designed rotating object placed near the laser beam. We show that such an apparatus is feasible (though not easy) to construct, present an example design, and calculate the signal that would be detectable by Advanced LIGO. This offers the first opportunity to measure space-time curvature effects on a laboratory distance scale.

PACS numbers: 04.80.Nn, 04.80.Cc, 04.50.Kd

Submitted to: *Class. Quantum Grav.*

1. Introduction

The general theory of relativity asserts that the familiar force of gravity is fundamentally a manifestation of the geometry of space-time, which is given curvature by massive objects. Many measurements of observable quantities which are influenced by space-time curvature have confirmed the validity of the Einstein Equivalence Principle—the foundation on which all metric theories of gravity are based—and the apparent correctness of general relativity as the specific metric theory [1]. Nevertheless, because of the importance of space-time and gravity to our understanding of the universe, opportunities for improved precision and new tests continue to be sought [2].

The most stringent tests of general relativity have been obtained from measurements of the time delay of an electromagnetic wave as it passes by a massive object. Although this effect is a natural consequence of the equivalence principle and the curvature of space, it was

not called out by Einstein and was first described by Irwin I. Shapiro in 1964 in the context of timing radar pulses reflected from Venus and Mars at superior conjunction [3]. The extra one-way time delay due to general relativity is

$$\delta t = 2 \frac{GM_{\odot}}{c^3} \ln \left(\frac{4r_1 r_2}{d^2} \right), \quad (1)$$

where M_{\odot} is the mass of the Sun, c is the speed of light, G is the gravitational constant, r_1 and r_2 are the orbital radii of the Earth and the target planet, and d is the distance of closest approach of the radar beam to the center of the Sun (assumed here to be much smaller than r_1 and r_2). For a radar reflection from Venus at the edge of the Sun, this amounts to a one-way time delay of 0.12 ms.

The time delay may be different in alternative theories of gravity. In the Parametrized Post-Newtonian (PPN) formalism for arbitrary metric theories [4, 1], the time delay is

$$\delta t = (1 + \gamma) \frac{GM}{c^3} \ln \left(\frac{4r_1 r_2}{d^2} \right). \quad (2)$$

In the $(1 + \gamma)$ factor, the 1 reflects the gravitational red-shift and is fixed for any metric theory of gravity, while the γ measures the net curvature of space produced by the mass along the path of the light or radio waves [1]. For general relativity, $\gamma = 1$, reproducing Shapiro's result. The possible deviation of γ from unity has been limited by radar ranging to Venus, Mars, and spacecraft, as well as by timing the radio pulses from isolated and binary pulsars [5, 6, 7, 8]; see [2] for a more recent summary of measurements. The most precise measurement was made using the Cassini spacecraft on its way to Saturn with a Doppler technique, yielding $\gamma - 1 = (2.1 \pm 2.3) \times 10^{-5}$ [9]. The same $(1 + \gamma)$ factor governs the angular deflection of light passing near the Sun, and very-long-baseline radio interferometry (VLBI) has been used to measure $\gamma - 1 = (-1.7 \pm 4.5) \times 10^{-4}$ [10]. Lunar laser ranging also is sensitive to γ in combination with other PPN parameters [11].

The Sun produces a measurable time delay at its edge despite the fact that most of its mass is located hundreds of thousands of kilometers away from the path of the radio beam. We may wonder whether smaller objects produce time delays for smaller separation distances according to the same model, *i.e.* the same effective value of γ . The PPN formalism does not allow for such a scale dependence, but there is no experimental evidence one way or the other for short distance scales. What time delay magnitude could we produce on a laboratory scale using a $\simeq 10$ -ton mass, say? As a back-of-the-envelope calculation, utilizing (2) with $M = 10^4$ kg, $r_1 = r_2 = 1$ km, and $d = 0.50$ m, we estimate that $\delta t = 8.2 \times 10^{-31}$ s. Remarkably, variations in that time delay due to *changes* in d can be detected using a suitable laser interferometer—for instance, one of the Advanced LIGO [12] gravitational-wave detectors—as we will discuss in section 2 below.

If the distance from the mass to the beam changes from d_{far} to d_{near} , the resulting change in time delay is

$$\Delta \delta t = (1 + \gamma) \frac{2GM}{c^3} \ln \left(\frac{d_{\text{far}}}{d_{\text{near}}} \right). \quad (3)$$

Thus, we can spin a massive object near the interferometer beam to modulate the time delay and then coherently integrate the signal over a long time period. Figure 1 is a sketch which

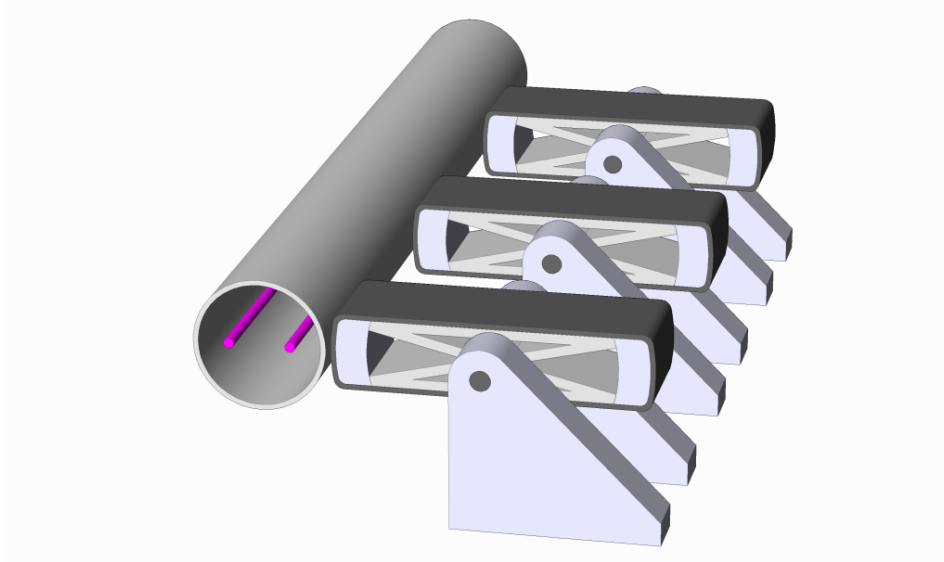


Figure 1. To produce a time-varying Shapiro time delay in one arm of a large interferometer, we envision placing several rotating masses next to the evacuated tube which encloses the laser beam. This figure shows the side-by-side beams of the two interferometers at the LIGO Hanford Observatory. The axis of rotation is parallel to the laser beams. Each section of the rotating mass system is supported by a bearing assembly in a separate vacuum enclosure (not shown); they rotate synchronously to produce a coherent effect on the laser beam.

illustrates this basic concept. In section 3, we discuss the design considerations for the rotating mass and present a specific example design which is sufficient to make an interesting measurement of the time delay, as described in section 4. We briefly examine several possible systematic effects and implementation issues in sections 5 and 6 and then conclude with a discussion of how future interferometers could make better measurements possible.

2. Laser Interferometers

Direct detection of gravitational waves [13] is the primary goal of modern interferometric gravitational wave detectors such as LIGO [14], VIRGO [15, 16], GEO600 [17], TAMA300 [18] and CLIO [19] which have successfully collected a few years of high-sensitivity data so far. Second-generation gravitational wave detectors now being designed and constructed—namely Advanced LIGO [12], Advanced Virgo [20] and the Large-scale Cryogenic Gravitational-wave Telescope (LCGT) [21]—will greatly extend the reach for gravitational wave signals. Each of these detectors is capable of measuring extremely small changes in the effective length difference of its two perpendicular “arms”, as would be induced by a passing gravitational wave. However, they can also be viewed as unique “laboratory” instruments capable of measuring induced displacements at the $\sim 10^{-23}$ m level, equivalent to time delays of $\sim 3 \times 10^{-32}$ s, for integration times of order one year.

This feature opens up new possibilities for fundamental science. While gravitational wave searches target signals with various durations, and either accurately-known or unknown

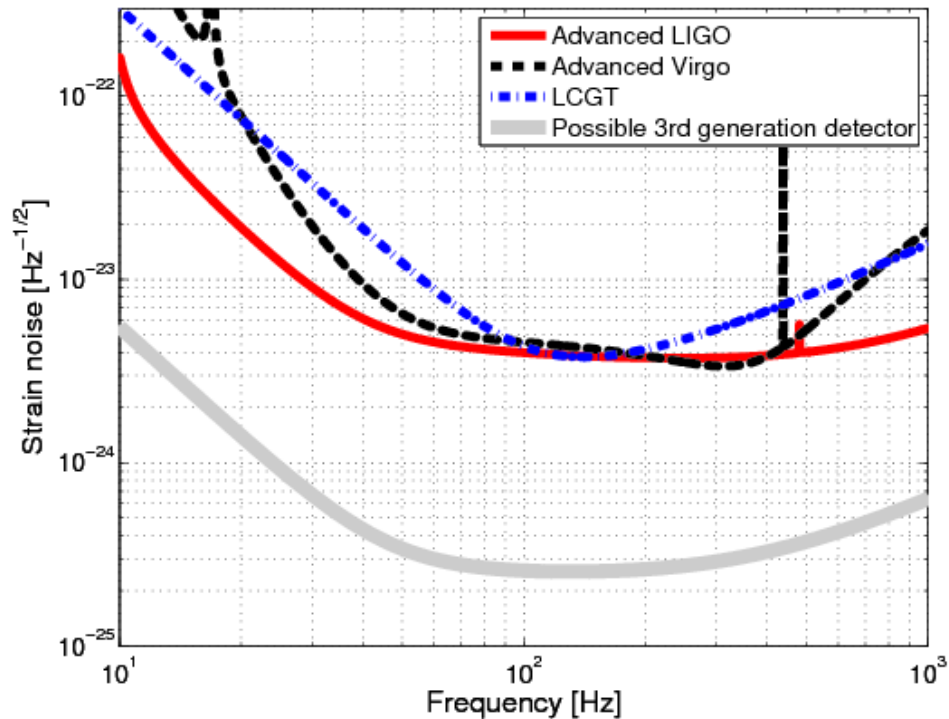


Figure 2. Nominal expected noise levels of second-generation gravitational wave detectors as a function of frequency, adapted from numerical models provided courtesy of the LIGO [22] and Virgo [20, 23] projects, and published by LCGT [21]. The Advanced LIGO curve is for the “zero-detuning, high power” configuration; see [22] for a brief summary of alternative configurations and caveats. The LCGT curve is for the “broadband RSE” configuration. The lowest strain noise is obtained for frequencies between about 70 and 300 Hz. Also shown is a representative noise curve for a possible third generation detector design [24], expected to have an order of magnitude lower noise and to have access to lower frequencies.

waveforms, precision experiments in which the light travel time in one of the interferometer arms is modulated at a given frequency in a well-controlled manner can enjoy all the benefit of sensitive lock-in experimental techniques and extended integration times.

Advanced LIGO will consist of three 4 km interferometric detectors at the two existing LIGO sites: the Hanford Observatory in Washington State (home to two detectors) and the Livingston Observatory in Louisiana. (A proposed alternative plan, to install one of the three Advanced LIGO detectors at the Gingin site in Australia, leaving just one at Hanford, is under consideration at the time of this writing.) The detectors will be installed beginning in 2011 and are expected to be fully operational around 2015, ultimately reaching an order of magnitude lower strain noise than the initial LIGO detectors.

The Advanced LIGO detector design has a beam splitter and suspended mirrors (test masses) at the ends of its orthogonal arms, as well as additional partially-transmitting mirrors, to form a power- and signal-recycled Michelson interferometer with Fabry-Perot arm cavities. A gravitational wave induces a time-dependent metric strain on the detector which changes the relative lengths of the arms. While acquiring scientific data, feedback to the mirror positions

and to the laser frequency keeps the optical cavities near resonance, so that interference in the light from the two 4 km long arms recombining at the beam splitter depends on the difference between the lengths of the two arms modulated by the signal to be measured. A photodiode senses the light, and a digitized signal is recorded. Then the data are calibrated and converted into a strain time series. The detectors have a sensitive frequency band extending from a few tens of Hz to a few kHz, as shown in figure 2, limited at low frequencies by seismic noise and radiation pressure noise and at high frequencies by laser shot noise. Third-generation detectors are envisioned to push the limits of ground-based interferometry and will likely be limited at low frequencies by Newtonian gravity-gradient noise [25].

3. Rotating Mass Design

Since laser interferometers like LIGO have essentially no sensitivity at DC, it is necessary to modulate the Shapiro delay by changing the effective distance between the beam and the relevant mass. The easiest way to achieve this is a rotating mass system. In this section we describe one possible design for a device with two “arms” extending from the rotation axis that would provide a Signal-to-Noise Ratio (SNR) of ~ 8 for one year of integration with Advanced LIGO. (There is no plan at this time to actually construct and operate such a device, but it could be considered as an addition to Advanced LIGO or another interferometer in the future.)

As indicated by (3), the geometry of the rotating mass setup enters only logarithmically into the Shapiro delay, while the mass enters linearly. The closest effective distance of the mass to beam, d_{near} , is constrained by their finite cross-sectional sizes. As a consequence it is hard to reduce the required mass by optimizing the rotating mass geometry. For the example design we assume a mass of 1.5×10^4 kg for each of the two arms.

One of the limiting factors is the tensile strength of the material holding the rotating mass together. This of course favors low spin frequencies, and therefore requires a laser interferometer with good low-frequency sensitivity. In the case of Advanced LIGO we would like to have the primary harmonic at about 50 Hz, well separated from known instrumental lines in the detector noise spectrum. Thus, a baseline design with two arms must rotate at 25 Hz. Note that this is still much slower than the inverse light travel time for all relevant distances; thus a static calculation of the Shapiro delay is still appropriate. A rotating mass system design with more arms would have a lower spin frequency, but in order to preserve the size of the variation of the Shapiro delay, one would have to increase the radius by the same factor. Since the whole rotating mass system needs to spin in vacuum and it must fit next to the beam tube we choose 1.5 m as the maximal practical rotating mass radius and stay with the conceptually simpler two-arm design and a 25 Hz spin frequency, even though one might win a factor of two in required tensile strength by going to 4 arms.

With these parameters the rotating mass structure needs to support a centrifugal force of about 6×10^8 N. A simple rectangular slab of steel, tungsten or titanium is not strong enough, and only a fraction of the mass would pass close to the laser beam. A better way to build a rotating mass system with the necessary strength is to concentrate the mass near

the ends of the arms, with a light-weight central support structure for suspension, and an outer shell of carbon fiber composite. Figure 3 shows a sketch of this rotating mass design, including the key dimensions. With a carbon fiber composite cross-sectional area of 1 m^2 (5 cm thickness on both sides and 10 m cumulative rotating mass length along the axis of rotation) this requires a tensile strength of 600 MPa. A composite such as HexTow IM9 from HEXCEL corporation [26], for example, provides a factor of 5 safety margin on this.

Another constraint on the geometry of the setup, specifically the length of the interferometer arms, comes from the direct gravitational coupling from the rotating mass to the test masses. A good place to put the rotating mass is near the middle of one interferometer arm. The test mass acceleration at the fundamental spin frequency f_{spin} cancels due to the symmetry of the rotating mass, while the acceleration variation at $2f_{\text{spin}}$ has amplitude

$$a = \frac{15 GMr^2(r+d)^2}{2 (L/2)^6} \quad (4)$$

where M is the mass of one arm, r is the rotating mass radius, d its minimal separation from the laser beam, and L is the interferometer arm length. For a 25 Hz spin frequency and including the acceleration of both test masses of the interferometer arm the length change at $f = 50 \text{ Hz}$ has amplitude

$$dx = \frac{240 GMr^2(r+d)^2}{\pi^2 f^2 L^6} \quad (5)$$

$$\approx \left(\frac{384 \text{ meter}}{L} \right)^6 \frac{2GM}{c^2}. \quad (6)$$

Since the size of the Shapiro delay is on the order of the Schwarzschild radius $2GM/c^2$ of one of the arm masses, divided by c , any laboratory-scale interferometer ($L \simeq 40 \text{ m}$ or less) would require an extremely precise cancellation mechanism. For the $L = 4 \text{ km}$ arm length of LIGO this coupling is down by more than 6 orders of magnitude.

4. Signal Analysis

For a given rotating mass, such as the one described in the previous section, it is straightforward to numerically calculate the gravitational potential U at every point in its vicinity. A light ray which passes near the rotating mass experiences a total time delay which is simply given by

$$\delta t = \int (1 + \gamma) U ds \quad (7)$$

where the integral is along the path of the light ray [1]. The light also experiences angular deflection during its passage, but for this system the deflection is only of order $\sim 10^{-22}$ rad. The slightly increased length of the path due to this deflection is quadratic in the angle, and thus has a negligible effect on the time delay calculation. Therefore we may take the light path to be straight in the \hat{z} direction (along the laser beam) and calculate the integrated time delay as a function of its transverse position when it passes by the rotating mass. Also, because the potential is additive, the spatial extent of the rotating mass in the \hat{z} direction does not matter;

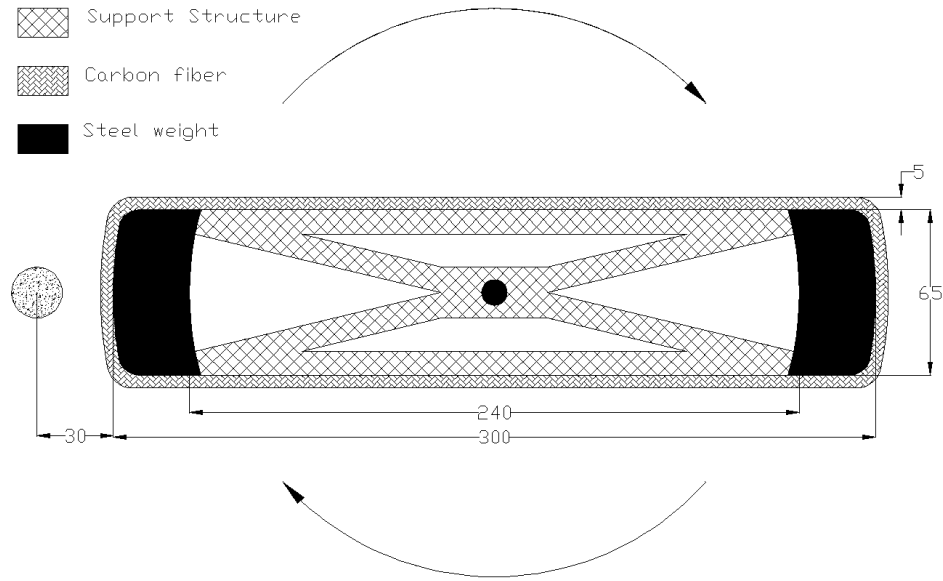


Figure 3. Cross-section of the example rotating mass system. All units are in cm. The support structure centered on the rotation axis is adequate to support the static weight of the steel weights, which represent most of the mass of the system. The carbon fiber epoxy composite outer envelope provides tensile strength when the system is spinning. The center of the laser beam is located 30 cm from the outer edge of the masses.

we can project all of its mass density to the x - y plane. Figure 4 shows contours of constant time delay (isochrones) around our example rotating mass design.

The time delay experienced by the light in the interferometer beam at any instant depends on the orientation of the rotating mass. As seen from the point of view of the rotating mass, the interferometer beam travels in a circle around the axis, as illustrated by the dashed lines in figure 4 for beams with closest-approach distances of 30 cm and 80 cm, representing the two interferometer beams at LIGO Hanford. The time delay at the center of the beam as a function of time is shown in figure 5 for one full rotation of the rotating mass. This is the signal which would appear in the interferometric data stream. Because the form of the signal is known accurately, it may be extracted from the data using lock-in techniques.

The signal is not purely sinusoidal because the distances from the different parts of the rotating mass are comparable to the size of the rotating mass. Figure 6 shows the Fourier components of the signal (for the nominal spin frequency of 25 Hz) superimposed on the expected sensitivity curve for Advanced LIGO assuming an integration time of one year. Based on this comparison, the fundamental frequency component at 50 Hz should be detectable with amplitude SNRs of 7.2 and 4.4, respectively, in the closer and farther beams. The first harmonic (at 100 Hz) should also be detectable in the closer beam with SNR of 2.3. Comparing these different measurements would test the consistency of the results with the expected form of the signal, while combining them in quadrature yields a total SNR of 8.7.

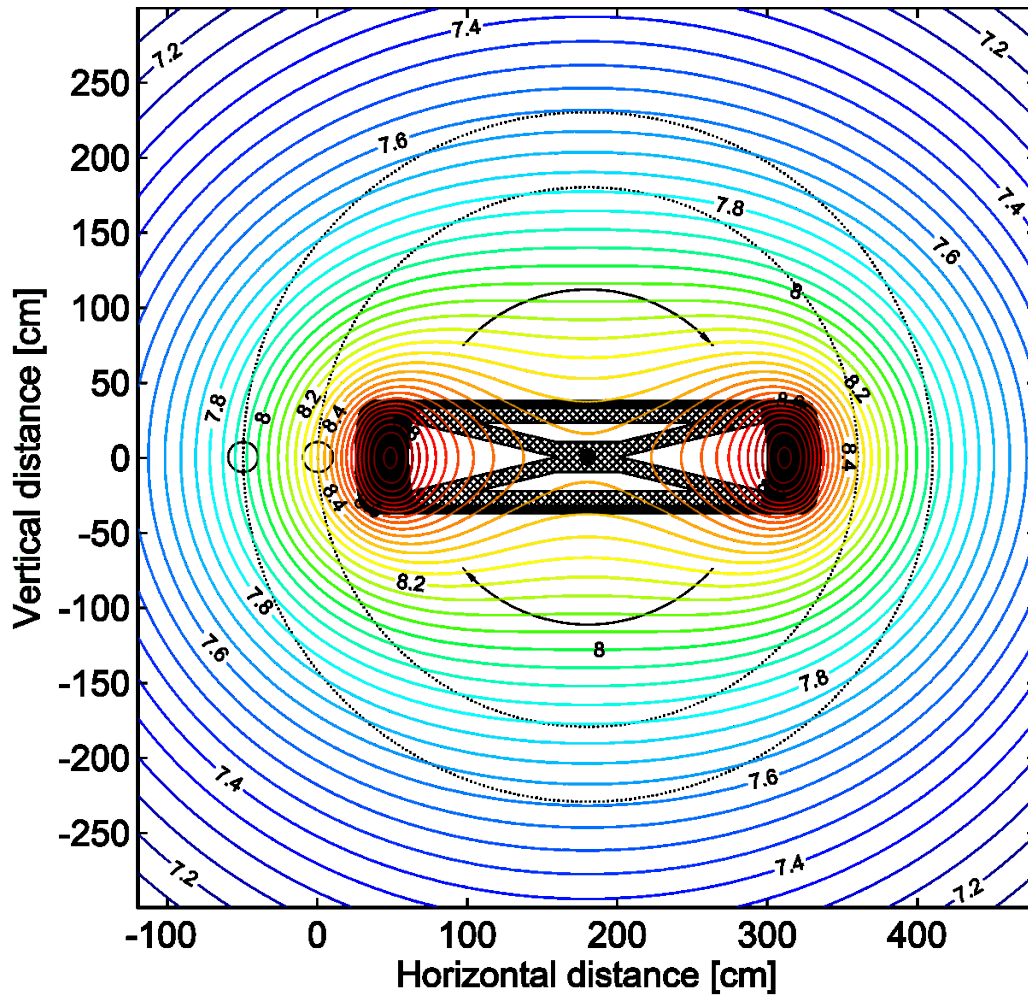


Figure 4. Shapiro time delay of the laser beam as a function of the position around the rotating mass. Note that the contour pattern rotates with the mass. The contour labels are in units of 100 yoctometers (10^{-22} m). The small black circles illustrate the relative size and position of the laser beams at the time of the closest approach. The large dotted circles trace out the positions of the centers of the laser beams relative to the rotating mass for a full revolution for the specific configuration discussed. The paths of the dashed circles through the isochrones map out the curves shown in figure 5.

5. Possible systematic uncertainties

To interpret the measured signal as being due to the Shapiro time delay, we must have sufficiently accurate knowledge of the geometry of the apparatus and must be able to rule out other possible systematic effects which could affect and/or fake the Shapiro delay signal. However, given that we only expect an SNR of ~ 8 above the instrument noise, we only need to limit these systematic effects to a few percent of the expected signal amplitude.

First, we must know the separation between the rotating masses and the interferometer beam to within a few percent, *i.e.* perhaps 1 cm. The rotating mass system parts can be machined and assembled with much tighter tolerances, and also measured precisely after

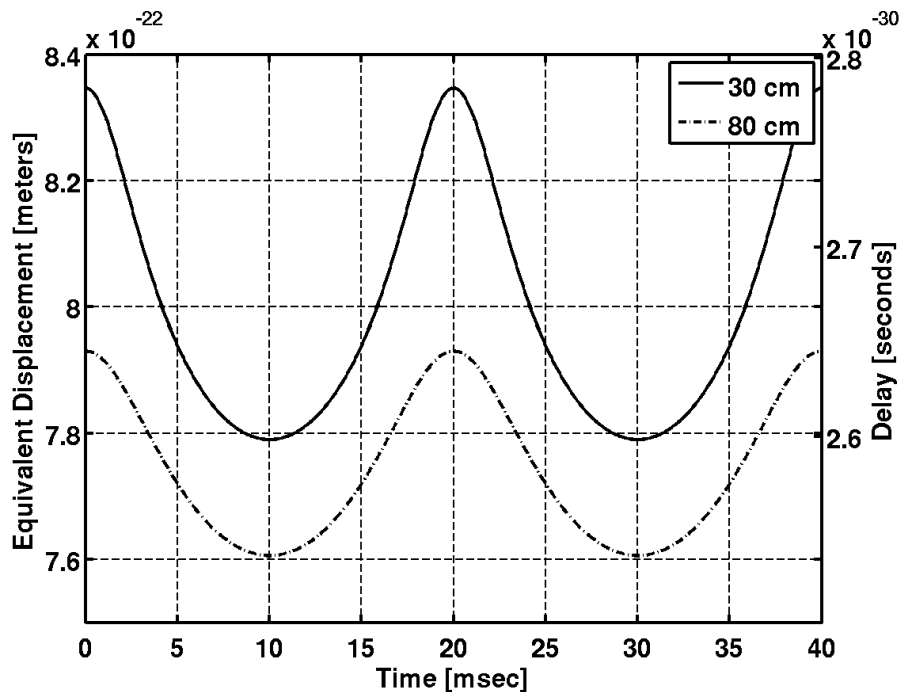


Figure 5. Shapiro time delay of the laser beam as a function of the time for one full rotation of the rotating mass system. The two traces correspond to laser beam positions 30 cm and 80 cm away from the outer edge of the rotating mass.

assembly. When spun up, the rotating mass system would stretch by about 5 mm due to the extreme tension on the carbon fiber composite outer layer; this should be taken into account in the data analysis and may not be known precisely (due to uncertainty in the bulk modulus of the carbon fiber composite) but would be a small correction. Knowledge of the interferometer beam position within its vacuum tube would be a greater challenge, but can probably be determined to 1 cm or better. The Advanced LIGO alignment system should keep the position of the beam stable to much better than 1 mm over the course of a year-long data run. There would also be a horizontal gradient in the time delay over the area of the interferometer beam, but the intensity-weighted mean delay (over the Gaussian beam profile) would be well-determined and the gradient is not expected to cause any other problems. Additionally, the diameter of the laser beam's vacuum tube may have to be reduced locally to allow the required close approach of the rotating mass to the laser beam.

It may be advantageous to minimize the length of beam tube devoted to the rotating mass system by placing synchronized rotating units on both sides of the beam tube. This also would reduce the time delay gradient over the area occupied by the laser beam. In the case of LIGO Hanford, rotating mass systems on both sides would produce equal time delays in both interferometers (but would only partly reduce the time delay gradient across each laser beam).

We must also consider parasitic coupling of the rotating mass system's motion to the interferometric signal through mechanisms other than the time delay. As mentioned in

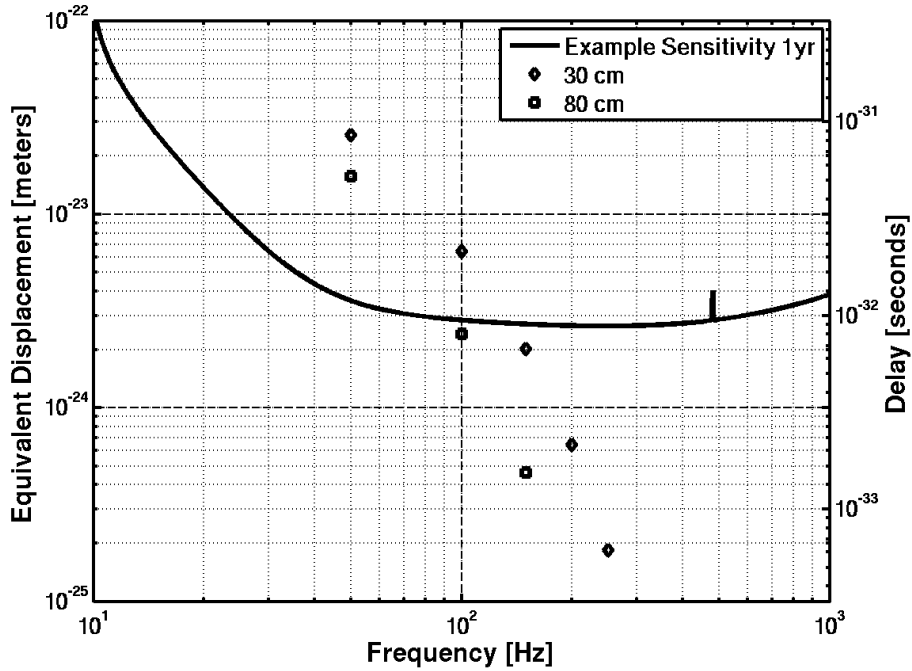


Figure 6. Fourier components of the Shapiro time delay signal. The diamonds and squares correspond to laser beam positions of 30 cm and 80 cm away from the outer edge of the rotating mass. Also shown is an example Advanced LIGO sensitivity curve, scaled for 1 year of integration time.

section 3, direct gravitational coupling to the test masses would be negligible due to the length of the interferometer arms. Electromagnetic interference from the motor driving the rotating masses should be negligible due to being so far away from the sensing electronics. Additionally one can use a gear so that the motor runs at a different frequency.

Another concern is local vibration of the interferometer beam's vacuum tube, directly excited by the time-varying gravitational field of the rotating mass system. This vibration would have a significant component at twice the spin frequency and could couple into the interferometric signal by modulating light scattered off the walls of the beam tube.

Baffles placed at an appropriate distance can sufficiently reduce the effects of light scattering. These baffles must be mechanically isolated from vibrations coming from either the beam tube or the ground.

The residual coupling from such baffles can also be estimated using (6), with an additional scattering factor.

$$dx_{\text{scat}} \approx \left(\frac{E_{\text{scat}}}{E_{\text{beam}}} \right) \left(\frac{384 \text{ meter}}{L} \right)^6 \frac{2GM}{c^2} \quad (8)$$

Thus placing the baffles a few hundred meters away from the rotating mass should provide sufficient isolation. Secondary scattering should also be analyzed, but that goes beyond the scope of this paper.

Such a massive rotating mass system, if even slightly unbalanced, would vibrate the

ground as it rotates. We should be able to tune the balance below the sensitivity level of seismometers at initial assembly. However, residual vibration might evolve due to aging or slow differential stretching of the rotating mass's carbon fiber composite layer when it is spun up to very high speeds. If the vibration is not sufficiently attenuated as it travels through 2 km of ground, it could shake the sensing optics and introduce a spurious signal. However, the vibrational signal would be generated primarily at the spin frequency and should be detectable with seismometers near the rotating mass systems and near the interferometer test masses. Thus a vibrational signal carried through the ground would largely be distinguishable from the time delay signal, which appears at twice the spin frequency and harmonics thereof.

We also note that any residual false signal due to vibrational coupling is likely to appear in the data with a phase different from what is expected from the relativistic time delay signal; this provides a useful consistency test.

6. Engineering considerations

Actual construction and operation of a rotating mass system like the one described in this paper would present several engineering challenges, but we believe that they could all be met with existing technologies. While detailed solutions are beyond the scope of this exploratory study, we can at least comment on the major issues.

In the example rotating mass system design, a total mass of $\simeq 30$ tonnes with a total length of 10 m must be supported reliably and spun with little friction. Rather than attempting to do that with a single assembly 10 m long, we imagine that it would be divided into several independent sections, each supported by multiple bearings to be able to tolerate the failure of a bearing. The sections would be rotated by independent motors. The rotation of each section would be monitored with a rotary encoder and fed back to the drive motor to maintain the desired spin frequency and phase. The rotation and drive force would also be monitored for signs of possible drive or bearing failure.

The kinetic energy of each rotating section would be of order 100–200 MJ, comparable to the energy in commercially available flywheel units used for energy storage [27]. Obviously, a structural failure must be avoided at all costs; the safety of the facility and personnel would be crucial considerations if this experiment is to be carried out.

7. Discussion

In this paper, we have explored the possibility of measuring the effects of space-time curvature over laboratory distance scales for the first time. We have found that it is technically feasible to make this measurement using the Advanced LIGO interferometers. However, it is far from easy. We had to resort to the use of high-tensile-strength composite materials to obtain a rotating mass system with sufficient mass and rotation speed to produce a measurable effect with an SNR of ~ 8 integrated over a year of data. This is sufficient to measure γ with a precision of $\sim 25\%$, which could distinguish between the cases $\gamma = 1$ and $\gamma = 0$, for instance.

Future interferometers could improve this type of measurement, especially if their low-frequency sensitivity is better [28] so that the mass can be rotated at a lower frequency. In particular, a design study is currently underway for a future underground “Einstein Telescope” [29] with projected sensitivity shown by the lowest curve in figure 2. That detector could support a Shapiro time delay measurement at a spin frequency of ~ 15 Hz that would be an order of magnitude better than the Advanced LIGO example presented in this paper. Besides the planned gravitational-wave interferometers, a dedicated interferometer could perhaps be used to make this time delay measurement. Although we cannot hope to approach the precision of the radar ranging measurements with this technique, it is interesting to be able to test gravity in an entirely different distance regime.

Acknowledgments

LIGO was constructed by the California Institute of Technology and Massachusetts Institute of Technology with funding from the National Science Foundation and operates under cooperative agreements PHY-0107417 and PHY-0757058. The authors are also grateful for the support of the National Science Foundation under grants PHY-0457528, PHY-0653421, PHY-0757957 and PHY-0757982; Columbia University in the City of New York; the University of Maryland; and the California Institute of Technology. We are indebted to many of our colleagues for fruitful discussions, in particular Daniel Sigg, Rainer Weiss, Rubab Khan and Zsuzsa Márka, and to Yoichi Aso for providing figure 1. We also thank an anonymous referee for helpful suggestions. This document has LIGO Document Number LIGO-P080029-v3.

References

- [1] Will C M 1993 *Theory and Experiment in Gravitational Physics* 2nd ed. (Cambridge: Cambridge University Press)
- [2] Will C M 2006 *Liv. Rev. Rel.* 2006-3
- [3] Shapiro I I 1964 *Phys. Rev. Lett.* **13** 789–91
- [4] Will C M and Nordtvedt K Jr 1972 *Astrophys. J.* **177** 757–74
- [5] Taylor J H and Weisberg J M 1989 *Astrophys. J.* **345** 434–50
- [6] Will C M 1990 *Science* **250** 770–6
- [7] Stairs I H, Arzoumanian Z, Camilo F, Lyne A G, Nice D J, Taylor J H, Thorsett S E and Wolszczan A 1998 *Astrophys. J.* **505** 352–7
- [8] Kramer M *et al* 2006 *Science* **314** 97–102
- [9] Bertotti B, Iess L and Tortora P 2003 *Nature* **425** 374–6
- [10] Shapiro S S, Davis J L, Lebach D E and Gregory J S 2004 *Phys. Rev. Lett.* **92** 121101
- [11] Williams J G, Turyshev S G and Boggs D H 2004 *Phys. Rev. Lett.* **93** 261101
- [12] Harry G M (for the LIGO Scientific Collaboration) 2010 *Class. Quantum Grav.* **27** 084006
- [13] Hughes S A, Márka S, Bender P L and Hogan C J 2001 *Proc. APS/DPF/DPB Summer Study on the Future of Particle Physics (Snowmass 2001)* ed N Graf, eConf C010630, P402, arXiv:astro-ph/0110349
- [14] Abbott B P *et al* 2009 *Rep. Prog. Phys.* **72** 076901
- [15] Acernese F *et al* 2008 *Class. Quantum Grav.* **25** 184001
- [16] Accadia T and Swinkels B L (for the VIRGO Collaboration) 2010 *Class. Quantum Grav.* **27** 084002
- [17] Grote H (for the LIGO Scientific Collaboration) 2010 *Class. Quantum Grav.* **27** 084003

- [18] Takahashi R *et al* (TAMA Collaboration) 2008 *Class. Quantum Grav.* **25** 114036
- [19] Yamamoto K *et al* 2008 *J. Phys.: Conf. Ser.* **122** 012002
- [20] The Virgo Collaboration 2009 *Advanced Virgo Baseline Design*; URL <https://pub3.ego-gw.it/itf/tds/file.php?callFile=VIR-0027A-09.pdf>
- [21] Kuroda K (on behalf of the LCGT Collaboration) 2010 *Class. Quantum Grav.* **27** 084004
- [22] Advanced LIGO Interferometer Sensing and Control Group 2010; URL <https://dcc.ligo.org/cgi-bin/DocDB/ShowDocument?docid=2974>
- [23] URL <http://www.cascina.virgo.infn.it/advirgo/>
- [24] Hild S, Chelkowski S and Freise A 2008 *Preprint* arXiv:0810.0604v2
- [25] Hughes S A and Thorne K S 1998 *Phys. Rev. D* **58** 122002
- [26] URL <http://www.hexcel.com>
- [27] Lazarewicz M and Rojas A 2004 *IEEE Power Engineering Society General Meeting 2004* vol 2 pp 2038–42
- [28] DeSalvo R 2004 *Class. Quantum Grav.* **21** S1145–54
- [29] Punturo M *et al* 2010 *Class. Quantum Grav.* **27** 084007